Gold bearing ore assays using 197Au(γ,n)196Au photonuclear reaction

ARTICLE *in* JOURNAL OF RADIOANALYTICAL AND NUCLEAR CHEMISTRY · JUNE 2014

Impact Factor: 1.03 · DOI: 10.1007/s10967-014-3239-2

3 AUTHORS, INCLUDING:

Valeriia Starovoitova

Idaho State University

20 PUBLICATIONS **42** CITATIONS

SEE PROFILE

J Radioanal Nucl Chem
DOI 10.1007/s10967-014-3239-2

Gold bearing ore assays using $^{197}Au(\gamma,n)^{196}Au$ photonuclear reaction

Sultan J. Alsufyani · Lauren R. Liegey · Valeriia N. Starovoitova

Received: 2 April 2014

Abstract We performed computational and experimental studies of the feasibility of the gold bearing ore assay utilizing the $^{197}Au(\gamma,n)^{196}Au$ photonuclear reaction. Gold bearing silicate samples were irradiated using bremsstrahlung produced by an electron accelerator with endpoint energies ranging from 25 to 40 MeV. ^{196}Au yield simulations were benchmarked and experimental results were in good agreement with the predictions. Optimum electron beam energy for photon activation analysis was found to be around 32 MeV which corresponded to a detection limit of 80 ppb. Two-hour gamma-spectroscopy measurements were repeated every 24 h and the optimum sample cooling time was found to be about 100–160 h.

Keywords Gold bearing ore assay · Photon activation analysis · Photoneutron production

S. J. Alsufyani · L. R. Liegey · V. N. Starovoitova
Idaho Accelerator Center, Idaho State University, 1500 Alvin Ricken Dr, Pocatello, ID 83201, USA

Present Address:
S. J. Alsufyani
Taif University, Makkah, Al-Huwayah, P.O. Box 888, Taif, Saudi Arabia

Present Address:
L. R. Liegey
Truman State University, 100 East Normal Avenue, Kirksville, MO 63501, USA

Present Address:
V. N. Starovoitova (✉)
Niowave Inc., 1012 N. Walnut St, Lansing, MI 48906, USA
e-mail: starvale@isu.edu

Introduction

Low concentrations of gold in geological samples typically require digestion and separation of gold from the associated base metals. Fire assay is the most common digestion technique; however, other methods, such as wet acid treatment, chlorination, and oxidation fusion are also used to transform the gold-bearing sample into a soluble complex suitable for further analysis. Combining digestion methods with spectrometric techniques, such as UV–VIS spectrophotometry, AAS, AES and ICP-MS for the examination of various materials have been described elsewhere [1–13].

The feasibility of using activation analysis for gold assaying has been already widely investigated. For example, neutron activation analysis (NAA) utilizing the $^{197}Au(n,\gamma)^{198}Au$ neutron capture reaction is a very sensitive method, but a typical sample weight for irradiation in a nuclear reactor is limited to less than a gram due to the high activities produced [14, 15]. Neutron sources can be used for NAA as well, but the sensitivity of such analysis is much lower [16]. Photon activation analysis (PAA) is another competitive technique with many advantages over the already existing methods suggested to determine the concentration of many noble metals, including gold. PAA has excellent sensitivity for gold by both isomeric state photoexcitation ($^{197}Au(\gamma,\gamma')^{197m}Au$) and photoneutron production ($^{197}Au(\gamma,n)^{196}Au$). The $^{197}Au(\gamma,\gamma')^{197m}Au$ reaction caused a lot of interest due to low electron beam energy requirements (threshold energy is 0.41 MeV) [17]. However, the short half-life of the produced metastable state (7.7 s) makes sample transfer and gamma-spectroscopy analysis challenging. The $^{197}Au(\gamma,n)^{196}Au$ reaction results in a relatively long-lived isotope with a half-life of several days and high cross-section, implying a high

Published online: 08 June 2014

Table 1 Possible photonuclear reactions with ^{197}Au resulting in gamma-emitting isotopes, their threshold energies, half-lives of the produced isotopes and energies of emitted gammas [18, 19]

Reactions	Threshold energy (MeV)	Half live of the produced isotope	Energies of emitted photons (strongest lines) (keV) and corresponding emission probabilities (I%)
Au-197 (γ,γ′) Au-197m	0.41	7.73 s	279.01 (73)
Au-197 (γ,n) Au-196	8.07	6.183 days	355.68 (88), 332.98 (23)
Au-197 (γ,n) Au-196m2	8.07	9.7 h	147.81 (43), 188.27 (38)
Au-197 (γ,n) Au-196m	8.07	8.1 s	84.66 (0.3)
Au-197 (γ,2n) Au-195	14.71	186.09 days	98.85 (11)
Au-197 (γ,2n) Au-195m	14.71	30.5 s	261.75 (68)
Au-197 (γ,3n) Au-194	23.08	38.02 h	293.55 (11), 328.45 (61)
Au-197 (γ, He-3) Ir-194	13.56	19.28 h	328.46 (13)
Au-197 (γ,He-3) Ir-194m2	13.56	171 days	482.83 (97), 328.45 (93), 482.83 (97)
Au-197 (γ,2p) Ir-195	14.04	2.5 h	98.85 (9)
Au-197 (γ,2p) Ir-195m	14.04	3.8 h	319.90 (13), 364.94 (13), 684.88 (13)

sensitivity of gold determination. The typical sample turnaround for the photoneutron technique is much longer in comparison with the photoexcitation method; however, it could be shortened further by sacrificing accuracy (e.g., lessening irradiation, decay, and counting times). The goal of this paper is to investigate gold bearing ore assay utilizing the ^{197}Au(γ,n)^{196}Au photonuclear reaction and finding optimum irradiation conditions to minimize the detection limit (DL) of gold in the ores.

Theory

Photon activation analysis

Over the last fifty years, photon activation techniques have been developed and used for nondestructive trace element analysis and applied to challenging questions in diverse fields ranging from provenance determination to assay of ore. Essentially, all of these techniques consist of two steps, starting with a high-energy photon irradiation, during which a small number of isotopes in the sample are transmuted by photonuclear reactions into radioisotopes. The secondary emissions from the decay of these radioisotopes are then detected, providing a radioisotope fingerprint that allows the identification of the original elements in the sample. With careful calibration of these two steps, the trace elements cannot only be identified, but also quantified.

The PAA process begins with an ore sample placed behind a bremsstrahlung radiator at the end of an electron accelerator. During the irradiation, electrons from the accelerator impinge on a radiator, which converts a fraction of the high-energy electrons to high-energy bremsstrahlung γ-rays. The resulting high-energy bremsstrahlung beam is forward-directed and highly penetrating, making it ideally suited for applications with thick, dense samples like mining ores. As the high-energy bremsstrahlung photons pass through the ore, they induce photonuclear reactions in its constituent isotopes.

After the irradiation, the sample is transferred to a position in front of a well shielded high-purity germanium (HPGe) detector which measures the intensity of the characteristic γ-rays emitted by the radioisotopes that were produced during the irradiation. Ultimately, these intensities are used for determining the concentration of the trace elements in the ore.

Natural gold contains only one isotope, ^{197}Au. However, high energy photons' interaction with ^{197}Au may result in many different gamma-emitting isotopes (including metastable states) which theoretically can be used for PAA. A list of possible photonuclear reactions, resulting in gamma-emitting isotopes and some of their properties, is given in Table 1.

The sensitivity of gold assay depends on the yield of the isotope, which, in turn, depends mostly on the photon flux, reaction cross-section, sample size and time of irradiation. The commonly used equation for photonuclear yield is [20]:

$$Y = N \int_{E_{\text{th}}}^{E_0} \phi(E) \cdot \sigma(E) \mathrm{d}E \tag{1}$$

where N is the number of target atoms, $\phi(E)$ is the photon flux, and $\sigma(E)$ is the reaction cross-section. The maximum sensitivity of gold assay can be achieved by utilizing the ^{197}Au(γ,n)^{196}Au reaction because it has the largest cross-section with maximum value of 550 mb at ~13.5 MeV

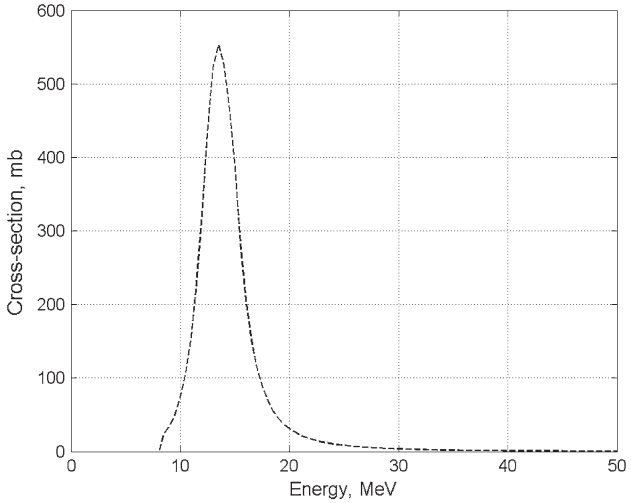

Fig. 1 ^{197}Au(γ,n)^{196}Au reaction cross-section adopted from the TENDL-2009 library [21]

(see Fig. 1). The rest of the reactions either require extremely high electron beam energy, or result in very short-lived radioisotopes, or have extremely low yield.

^{196}Au emits different energy gammas, the most prominent being at 356 keV (its branching ratio is 87 %). Other energies include 333 keV (23 %), 426 keV (7 %) and some other energies with even lower branching ratios. For the purpose of PAA, the 356 keV line in gamma-spectrum was used (Fig. 2).

Detection limit

To find the DL, we used a single measurement-to-noise ratio approach, which basically compares the signal to the background in the vicinity of the signal. To a 95 % confidence level, the DL can be found as [21]:

$$\mathrm{DL} = \frac{2 \cdot \mathrm{SD} \cdot C}{Y} \tag{2}$$

where C is the concentration of the isotope of interest, SD is standard deviation of the background in the vicinity of the peak in a gamma-spectrum, and Y is the yield of the isotope of interest or area of the peak in the gamma-spectrum. Figure 2 shows an example of the gamma-spectrum of ^{196}Au with different regions of the spectrum labeled.

To obtain the yield and standard deviation, two programs were written using MATLAB software. Yield was found by integrating the area under the peak and subtracting the background. Standard deviation was calculated according to the following equation:

$$\mathrm{SD} = \sqrt{\sum_{i=1}^{n} \frac{(x_i - \bar{X})^2}{n}} \tag{3}$$

where n is the total number of channels, $\bar{X}$ is the mean of the counts, and x_i is number of counts corresponding to ith channel.

Uncertainties in DL were determined using the general error propagation formula:

$$\frac{\delta_{\mathrm{DL}}}{\mathrm{DL}} = \sqrt{\left(\frac{\delta_{\mathrm{SD}}}{\mathrm{SD}}\right)^2 + \left(\frac{\delta_C}{C}\right)^2 + \left(\frac{\delta_Y}{Y}\right)^2} \tag{4}$$

where

$$\frac{\delta_{\mathrm{SD}}}{\mathrm{SD}} = \frac{\sqrt{\left(\frac{1}{n}(x_i - \overline{X})\delta_{x_i}\right)^2 + \left(\frac{1}{n}(x_i - \overline{X})\delta_{\overline{X}}\right)^2}}{\mathrm{SD}^2} \tag{5}$$

and

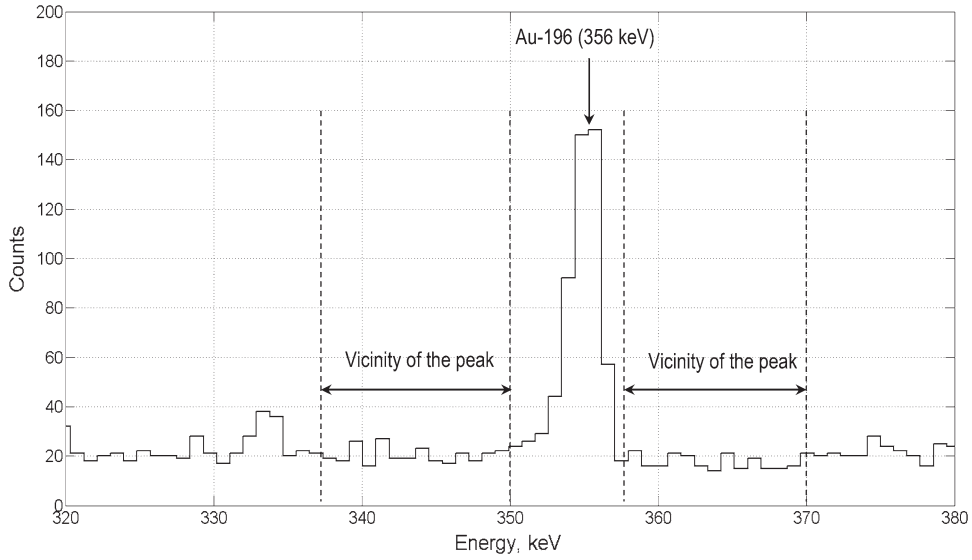

Fig. 2 A part of the gamma-spectrum showing 356 keV line used for measuring ^{196}Au yield and for finding detection limit. Note that 333 keV line while present cannot be distinguished from the background due to its low emission probability and thus cannot be used for the analysis

$$\frac{\delta_C}{C} = \sqrt{\left(\frac{\delta_{M_i}}{M_i}\right)^2 + \left(\frac{\delta_{M_{\mathrm{TOT}}}}{M_{\mathrm{TOT}}}\right)^2} \quad (6)$$

The last term in Eq. 4, δ_Y/Y, was found using built-in fitting function in the MPA-NT Software used for gamma-spectroscopy.

The DL depends on several parameters, including electron beam energy, time of irradiation and cooling, and sample dimensions and composition. In this work we are addressing two of the issues, namely energy and time of cooling. The irradiation energy must be sufficiently above the photonuclear reaction threshold to produce a sufficient population of the radioisotope of interest. However, the irradiation energy must be sufficiently low to prevent excessively high backgrounds. The reaction threshold for this reaction is 8.1 MeV and initially it increases rapidly as seen in Fig. 1. Hence irradiation energies under $\sim$8 MeV do not produce any ^{196}Au because there is no overlap between the bremsstrahlung flux and the cross section. Like all photonuclear reactions, the production of ^{196}Au can be increased by increasing the bremsstrahlung endpoint energy in order to increase the overlap of the flux with the cross-section and the overall intensity of the beam. Of course, larger energies can increase the background, so finding optimum energy is essential for each reaction.

After the irradiation, all radioactive isotopes produced in the ore sample decay. As cooling time increases the activity of ^{196}Au decreases. However, the background activity drops as well. Again, finding the optimum time when the "signal-to-background ratio" is at its maximum is important for minimizing the DL. Obviously, both optimum energy and optimum cooling time depend on the ore composition and gold concentration within it.

Description of the experiment

This project was completed at the Idaho Accelerator Center (IAC), a unique research facility operated by Idaho State University (ISU) using an S-band 48 MeV linac, consisting of two accelerating sections. The first section is the standing wave linac, which is designed to accelerate electrons from the electron gun up to 25 MeV. The second accelerating section, SLAC traveling wave linac, can accelerate the electron beam to the maximum energy of 48 MeV. The average current can vary from 10 μA to 0.5 mA, and pulse width can vary from 100 ns to 8 μs. The maximum power is 10 kW. Four different energies were used for irradiation: 25, 30, 35, and 40 MeV.

Both optimum energy and optimum cooling time depend on the ore composition and gold concentration within it. However, most gold bearing ores contain quartz and other light-colored minerals. To find the optimum irradiation conditions we prepared an artificial sample by loading sand (SiO_2) with known amount of $AuCl_2$ solution. Five identical samples were prepared using about 8 g of sand and 50 μg of gold. The sand-gold mix was placed in $\sim$30 g alumina crucibles, so that the net gold concentration in samples was between 1 and 1.5 ppm.

For irradiation, the samples were placed right behind a 4.5 mm thick water-cooled tungsten converter in a specially designed target holder. For each sample, the electron beam power was 500 W and time of irradiation was 30 min, so the electron beam energy was the only variable for the experiment. After irradiation, the samples were transferred into a shielded counting room where their gamma-spectra were obtained using a high purity germanium (HPGe) detector setup, consisting of a liquid nitrogen cooled detector, a 4.7 kV voltage supply, a charge-sensitive preamplifier, an amplifier, a multichannel analog–digital converter (ADC), and a computer with MPA-NT software. The detector had been calibrated using numerous point sources including Mn-54, Cs-137, Co-60, Cd-109, Ba-133, and others. Detector efficiency curves were created for several chosen distances from the detector so that actual activity of ^{196}Au could be measured. Mass-attenuation and self-shielding of the samples had been modeled and accounted for.

Results and discussion

^{196}Au yield

To estimate the time necessary to produce reasonable activity for a given electron beam energy and power, MCNPX simulation studies were performed. MCNPX is a general purpose particle transport Monte Carlo code developed by the Los Alamos National Laboratory [22]. Photon yield dependencies on beam energy and accelerator power were studied by allowing electron/photon transport and switching on the photonuclear physics flag in the PHYS:P card. ^{196}Au yields were determined by multiplying bremsstrahlung fluxes by TENDL-2009 photonuclear cross-sections and performing the integral (1) utilizing FM tally multipliers.

Experimental measurements of ^{196}Au yields from irradiation of beams of different energies were done using the gamma-spectroscopy setup described above. The detector efficiency for 355.6 keV photons for the position used for measurements (about 1 m away from the nozzle of the detector) was found to be

$$\eta = 7.034 \times 10^{-5} \quad (7)$$

To roughly estimate mass attenuation of gold by the sample (sand and crucible) we performed a number of simulations.

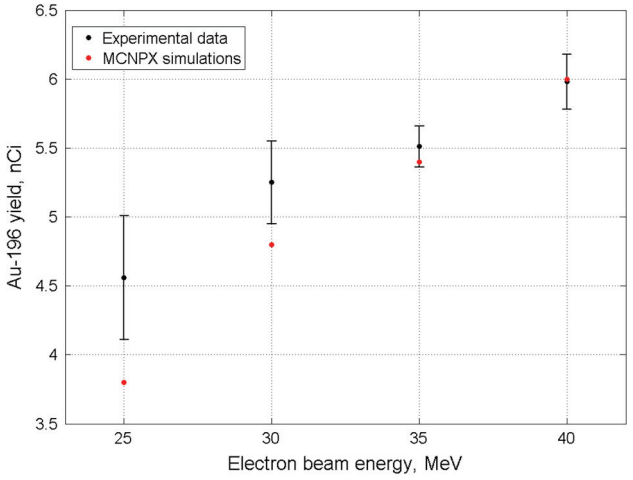

Fig. 3 Experimental values (*black*) and Monte-Carlo simulations (*red*) of ^{196}Au yield for different electron beam energies

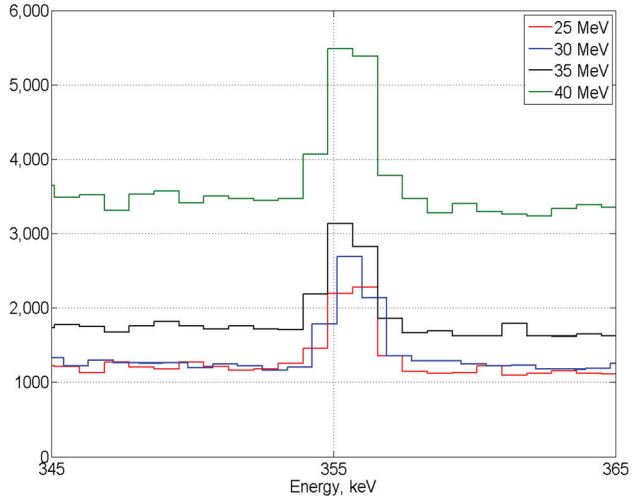

Fig. 4 Raw gamma-spectra taken 24 h after the irradiation using different electron beam energies

First, we modeled the distribution of ^{196}Au atoms inside the sample using MCNPX code and generated a distribution of distances photons had to travel through to reach the detector. Using mass-attenuation coefficients for sand and alumina we found that the apparent intensity "seen" by the detector was about 0.87 of the actual intensity generated inside the sample. Thus, yield measurements from the gamma-spectrometry experiment were corrected by this factor.

Measurements of ^{196}Au yield were found to be in good agreement with Monte-Carlo simulations (see Fig. 3). Slight disagreement between experimental and theoretical data can be explained by higher electron beam energy spread for lower energies and uncertainty in the cross-section function.

Detection limit measurements

The four spectra used for experimental measurements of ^{196}Au yields from irradiation of beams of different energies are shown in Fig. 4. It can be clearly seen that the 40 MeV spectrum has the highest ^{196}Au peak, but also the highest background. As the electron beam energy decreases, both the 355.6 keV peak and the background drop. We used the same spectra for the DL calculations, which were carried out according to Eq. 2. The uncertainty was calculated according to Eq. 4 and was found to be 5–8 % for all the data. Even though we only have four data points, the difference in the DL values is significant. Clearly, the optimum energy for our samples was around 30 MeV (see Fig. 5).

In addition to finding the optimum energy of irradiation, we were looking at the optimum cooling time of the sample. As time goes on, the background decays and so

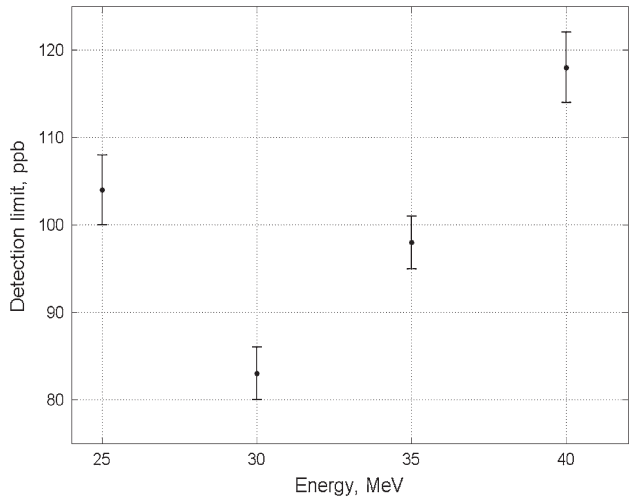

Fig. 5 Detection limit values as a function of electron beam energy. Optimum energy is about 30 MeV

does the peak of interest. To find the optimum time when the "ratio" of the peak to the standard deviation of the background is the highest, we used one of the irradiated samples, namely a sample irradiated at 40 MeV due to its maximum activity compared to the other three samples. We obtained numerous gamma-spectra performing the measurements every 24 h. The duration of each measurement was 2 h. The results of the measurements show a clear minimum in DL values around 100–160 h from the end of irradiation (Fig. 6). Thus by waiting for a few days for background to decay, the DL can be reduced by about a factor of three.

Note that the ^{196}Au half-life is 6.2 days and the irradiation period we used (30 min) was not long enough to saturate the ^{196}Au population. It would take several weeks

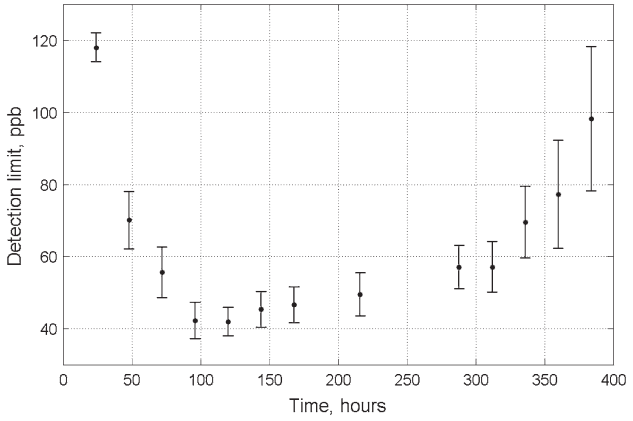

Fig. 6 Detection limit as a function of cooling time. Sample was irradiated for 30 min using 40 MeV electron beam

(4–5 half-lives) to reach 90–95 % of maximum possible yield, which is not practical. Furthermore, as can be seen from Fig. 5, the optimum cooling period between the irradiation and detection period is about 4 days. So for the highest sensitivity and lowest possible DL, a 4–5 day cooling period should follow a 25–30 day irradiation. Instead, it makes much more sense to set irradiation and detection periods by balancing the desired sensitivity with the sample throughput requirements of the application. If timing is an issue, a shorter irradiation and cooling time can be employed with the drawback of lower sensitivity and higher DL, and the whole ore assaying process can be accomplished in under 48 h.

Conclusions

Photon activation analysis of gold bearing ores based on the photoneutron production reaction $^{197}Au(\gamma,n)^{196}Au$ and measurements of ^{196}Au isotope yield ($T_{1/2} = 6.2$ days, $E_\gamma = 355.6$ keV) has been described. The deep penetration of the high energy bremsstrahlung of 25–40 MeV enables the irradiation of a large sample mass, on the order of hundreds of grams or even a few kilograms, potentially decreasing the need for highly homogenized ore samples. Furthermore, particulate size or water content of the ore samples is not important to the photonuclear reactions, potentially eliminating a number of processing steps required in sample preparation. In addition to assaying gold, these photonuclear techniques can detect and quantify a large variety of additional elements in ore samples, thereby providing a wealth of additional mineralogical information in a single simple assay.

Our measurements of ^{196}Au yields as a function of electron beam energy were in excellent agreement with the Monte-Carlo simulation results. It was shown that the DL is a function of electron beam energy as well as a function of cooling time. The optimum energy was found to be around 30 MeV and the optimum cooling time to be between 100 and 160 h. Both optimum irradiation time and optimum cooling time are impractical, so compromises should be made between the time of assay and sensitivity of the technique.

We have not addressed matrix effects, which start playing an important role as the size and mass of the sample increases. The background that limits the gold sensitivity normally stems from the decay of radioisotopes produced by photonuclear reactions with constituents in the ore that are not of primary interest. It is known that uranium, thorium, and other elements which may make up a sample increase the DL for real ores. Not only their natural activity, but above all, the continuum caused by bremsstrahlung of the β^--emitters from the uranium and thorium photofission increases the background in the spectra. Also, as the size and mass of the ore sample increases, absorption starts to play an important role. Hence the DL and optimal irradiation/detection parameters can change with ore type, mass, and size.

Finally, modifying the gamma-spectroscopy setup can significantly improve the sensitivity of the analysis. For example, using an NaI detector might be more advantageous than using an HPGe detector due to the higher photopeak counting efficiency of scintillation detectors. The low resolution of the NaI detector would not be a problem if no spectral interference is expected. However, if an activated sample emits photons with energies close to 356 keV, or if the goal of the analysis is to detect not only gold, but also other elements, then high resolution semiconductor detectors will be preferred. Further modifications of the gamma-spectrometry system might include adjustments of electronic pulse processing devices, additional shielding, and Compton suppression setups.

References

1. Van Loon JC, Barefoot RR (1991) Determination of the precious metals. Selected instrumental methods. Wiley & Sons, Chichester
2. Dominy SC, Annels AE, Johansen GF, Cuffly BW (2000) General consideration of sampling and assaying in a coarse gold environment. Trans Inst Min Metall 109:B145–B167
3. Haffty J, Riley LB, Goss WD (1977) A manual on fire assaying and determination of the noble metals in geological materials. USGS Bulletin 1445, Washington
4. Jackson SE, Fryer BJ, Gosse W, Healey DC, Longerich HP, Strong DF (1990) Determination of the precious metals in geological materials by inductively coupled plasma-mass spectrometry (ICP-MS) with nickel sulfide fire-assay collection and tellurium co-precipitation. Chem Geol 83:119–132
5. Juvonen MR, Bartha A, Lakomaa TM, Soikkeli LA, Bertalan E, Kallio EI, Ballók M (2004) Comparison of recoveries by lead fire

assay and nickel sulfide fire assay in the determination of gold, platinum, palladium and rhenium in sulfide ore samples. Geostand Geoanal Res 28:123–130
6. Balaram V, Mathur R, Satyanarayanan M, Sawant SS, Roy P, Subramanyam KSV, Kamala CT, Anjaiah KV, Ramesh SL, Dasaram B (2012) A rapid method for determination of gold in rocks, ores and other geological materials by F-AAS and GF-AAS after separation and preconcentration by DIBK extraction for prospecting studies. MAPAN J Metrol Soc India 27(2):87–95
7. Law SL, Green TE (1969) Solvent extraction in the presence of emulsion-forming residues. Application to the atomic absorption determination of gold in low-grade ores. Anal Chem 41(8): 1008–1012
8. Kasrai M, Fozoonmayeh L, Payrovan H (1988) Quantitative determination of gold in ore using energy-dispersive XRF spectrometry. X-Ray Spectrom 17(6):219–222
9. Hausen D, Odekir J (1991) XRD mineralogic logging of drill samples from gold and copper mining operations. Ore Geol Rev 6:107–118
10. Date AR, Davis AE, Cheung YY (1987) The potential of fire assay and inductively coupled plasma source mass spectrometry for the determination of platinum group elements in geological materials. Analyst 112:1217–1222
11. Resano M, McIntosh KS, Vanhaecke F (2012) Laser ablation-inductively coupled plasma-mass spectrometry using a double-focusing sector field mass spectrometer of Mattauch-Herzog geometry and an array detector for the determination of platinum group metals and gold in NiS buttons obtained by fire assay of platiniferous ores. J Anal At Spectrom 27(1):165–173
12. Marinenko J, May I (1968) Fluorometric determination of gold in rocks with Rhodamine B. Anal Sci 40(7):1137–1139
13. Balcerzak M (2002) Sample digestion methods for the determination of traces of precious metals by spectrometric techniques. Anal Sci 18:737–750
14. Randa Z, Spasek B, Mizera J (2007) Fast determination of gold in large samples of gold ores by photoexcitation reactions using 10 MeV bremssrauhlung. J Radioanal Nucl Chem 271(3):603–606
15. El-Bahi SM, Sroor A, Abdel-Haleem AS (1999) Application of neutron activation analysis technique for gold estimation in mines in southern Egypt. Appl Radiat Isot 50(3):627–630
16. Asif M, Parry SJ, Malik H (1992) Instrumental neutron activation analysis of a nickel sulfide fire assay button to determine the platinum group elements and gold. Analyst 117:1351–1353
17. Jarzemba MS, Weldy J, Pearcy E, Prikryl J, Pickett D (1999) Experimental determination of detection limits for performing neutron activation analysis for gold in the field. Nucl Sci Eng 133(3):335–341
18. IAEA-TECDOC (2000) Handbook on photonuclear data for applications. IAEA, Vienna
19. Segebade CR, Weise HP, Lutz GJ (1988) Photon activation analysis. Walter de Gruyter, Berlin. ISBN 3-11-007250-5
20. Koning AJ, Rochman D (2009) TENDL-2009: "Consistent TALYS-based evaluated nuclear data library including covariance data". Nuclear Research and Consultancy Group, Petten
21. Jenkins Ron (1999) X-ray fluorescence spectrometry, 2nd edn. Wiley, New York
22. Pelowitz D (ed) (2008) MCNPX user's manual, version 2.6.0, LA-CP-07-1473. Los Alamos National Laboratory